

Microscopic observation of shear-mode fatigue crack growth behavior under the condition of continuous hydrogen-charging

Y Akaki¹, T Matsuo^{2,3}, Y Nishimura⁴, S Miyakawa⁴ and M Endo^{2,3}

¹Graduate School of Engineering, Fukuoka University, 8-19-1 Nanakuma, Jonan-ku, Fukuoka 814-0180, Japan

²Development of Mechanical Engineering, Fukuoka University, 8-19-1 Nanakuma, Jonan-ku, Fukuoka 814-0180, Japan

³Institute of Materials Science and Technology, Fukuoka University, 8-19-1 Nanakuma, Jonan-ku, Fukuoka 814-0180, Japan

⁴Materials Engineering R&D Division, DENSO CORPORATION, Japan, 1-1 Syowa-cho, Kariya, Aichi 448-8661, Japan

E-mail: tmatsuo@fukuoka-u.ac.jp

Abstract. Rolling bearings facilitate the smooth motion of moving mechanical transmission devices substantially reducing the energy loss. However, flaking failure caused in bearings by rolling contact fatigue can crucially deteriorate the integrity of an overall mechanical system composed using bearings. It is understood nowadays that this phenomenon is intimately associated with shear-mode (Mode II and III) fatigue crack growth caused by cyclic shear stress in the presence of large compression. Further, a problem has become of importance that the premature flaking in ball bearings could be caused by the assistance of the penetration of hydrogen into material during the operation. In this study, torsional fatigue test of a bearing steel (JIS SUJ2) was performed by using a newly-developed method of continuous hydrogen-charging. Based on the microscopic observation, it was found that continuous hydrogen-charging had an influence on the shear-mode fatigue crack growth behavior in the high-cycle fatigue regime and reduced the threshold level.

1. Introduction

White structure flaking (WSF) is a typical failure frequently observed in rolling bearings used in automotive components, wind turbine gearboxes, etc, which is attributed to the crack growth from a surface or subsurface inclusion under the combination of cyclic shear stress and heavy compressive stress. Some previous studies [1-10] reported that WSF could be caused by invasion of the hydrogen derived from decomposition of lubricant in operation. In order to understand the essential mechanism of WSF, it is necessary to clarify the effect of hydrogen on the shear-mode fatigue crack growth behavior and the threshold condition, in particular for a small crack of a few millimeters or smaller in size that determines the rolling contact fatigue strength. However, there is only a few researches [10] that quantitatively investigate the growth behavior of a small sized shear mode fatigue crack. Especially, there is no study on the *high-cycle* fatigue in hydrogen environment because a problem had been left that hydrogen will emit from the specimen during fatigue test.



In our previous study [11], an easy-to-use as well as effective method was newly developed to investigate the shear-mode fatigue crack growth behavior in the presence of hydrogen. The developed method demonstrated that hydrogen had an influence on the shear mode fatigue crack growth behavior in the *low-cycle* fatigue regime. However, in order to ensure the safety in long-term use of rolling bearings, the *high-cycle* fatigue property in the presence of hydrogen is also an important issue to be addressed. In this study, the effect of hydrogen on shear mode fatigue crack growth behavior in the regime of high-cycle fatigue was investigated by utilizing the continuous hydrogen-charging (H-charging) method developed in the previous study [11].

2. Experimental set-up

2.1 Material and specimen

The material used in this study was a bearing steel, JIS-SUJ2, which is substantially the same material used for the ball in a ball bearing. The shape and dimensions of specimen are shown in Figure 1. To circulate an H-charging solution, a through-hole of 2 mm in diameter was introduced coaxially with the specimen axis. Also, a blunt notch with the gage length of 2 mm was introduced to localize the crack initiation site and to facilitate the observation of fatigue crack growth. The surface of specimen was finished by alumina-buffing following polishing with an emery paper up to #2000. Then, electro polishing was conducted to remove a thin worked layer with residual stress. The residual stress measured by the X-ray diffraction method was within ± 30 MPa.

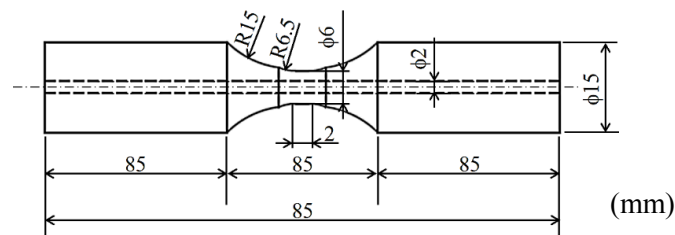
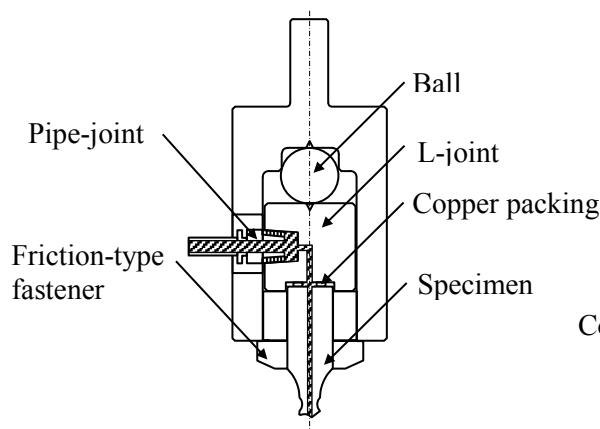


Figure 1. Fatigue test specimen.

2.2 Continuous hydrogen-charging method [11]

Continuous H-charging was performed by circulation of an aqueous solution of 20 mass% NH_4SCN in a specimen. The mechanism of hydrogen circulation is shown in Figures 2 and 3. This procedure was started 48 hours prior to the fatigue test under the H-charging condition. The hydrogen-charging solution was exchanged within 3 days monitoring the pH value to maintain a sufficient hydrogen supply to the specimen during fatigue test.



▨ Flow of H-charging solution

Figure 2. Specimen and fixture with channel of H-charging solution [11].

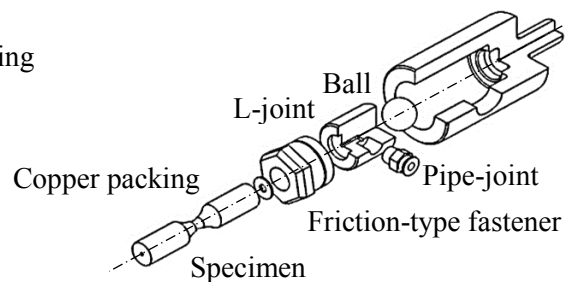


Figure 3. 3D illustration of components [11].

2.3 Fatigue test procedure

Fatigue test was carried out in air at room temperature by a servo-hydraulic combined axial/torsional loading fatigue testing machine. The frequencies were $f = 20$ Hz for testing under the non-charging condition and $f = 2$ Hz for testing under the H-charging condition. The stress ratio was $R = -1$. A statically-applied compressive axial stress of $\sigma_s = -1200$ MPa was superposed on the cyclic torsion to suppress the Mode I crack branching. The shear stress with a nominal amplitude of $\tau_a = 900$ MPa was initially applied to the specimen under the non-charging condition. The shear stress amplitude, τ_a , was thereafter decreased in a stepwise manner with increase in the crack length. In this study, when the fatigue crack growth rate, da/dN , became less than 10^{-11} m/cycle over an additional 10^6 cycles after the nominal shear stress amplitude had been decreased, the crack was regarded as a non-propagating crack. The critical value of τ_a was defined to be the threshold stress, τ_{th} , for crack propagation. After the non-propagation condition was satisfied under the non-charging condition, the testing condition was switched from non-charging to H-charging condition; namely, internal circulation of hydrogen-charging solution in the specimen was undertaken. The fatigue test under the H-charging condition was conducted at the same stress amplitude at which the non-propagation of a crack was observed under the non-charging condition. Surface cracks were observed by the replica method at every scheduled number of cycles to measure the crack length.

3. Results and discussion

The fatigue test was conducted using a single specimen according to the following sequence:

- (1) The test was initially performed under the non-charging condition at a high stress amplitude of $\tau_a = 900$ MPa to generate shear-mode fatigue cracks on the specimen surface, cf. Figure 4.
- (2) The stress amplitude was changed toward the threshold level in a stepwise manner, cf. Figures 5 and 6.
- (3) When the threshold level was found, i.e. the crack can be regarded as virtually stopping propagation, then the environmental condition was switched from non-charging to H-charging to investigate the effect of hydrogen-charging on the near-threshold growth behavior of a shear-mode fatigue crack, cf. Figure 7.

At step (1), the fatigue test at $\tau_a = 900$ MPa is in the regime of high-stress, low-cycle fatigue. A number of small fatigue cracks initiated on the specimen surface. The origin of crack initiation was mostly at the inclusions elongated in the axial direction. Figure 4 shows a typical process of the

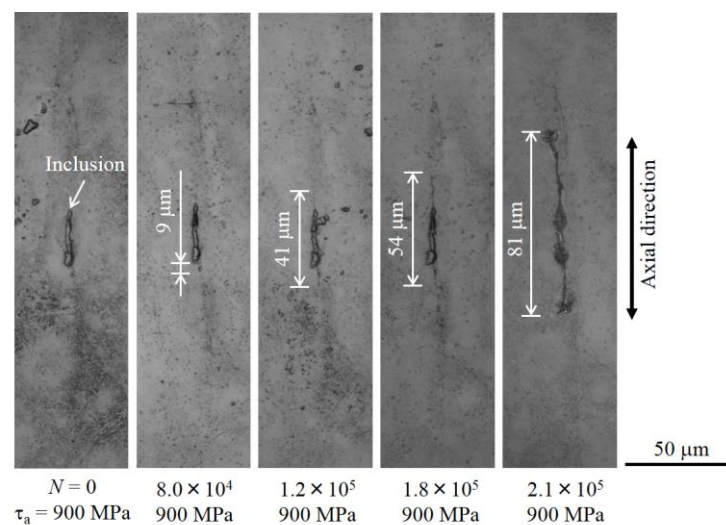


Figure 4. Shear-mode crack initiation and early growth behavior under non-charging condition. ($\sigma_s = -1200$ MPa $\tau_a = 900$ MPa, $f = 20$ Hz)

initiation and early growth of a shear-mode fatigue crack. The crack, initiated at a long shallow notch formed by dropping-off of inclusion, grew as a shear-mode crack in the axial direction. This crack was a leading crack with the maximum length throughout the investigation and therefore, its behavior was continuously observed afterward. In the previous study [11] in which a fatigue test was conducted under the identical test condition except for applying a little greater constant stress amplitude of $\tau_a = 1000$ MPa, the similarly-initiated crack with the maximum length grew maintaining a clear shear-mode feature up to a length of 256 μm , then caused a typical Mode-I crack branching oriented at an angle of about 45° with respect to specimen axis.

At step (2), after the stage of the far-right figure in Figure 4, the stress was continuously changed to smaller values step by step to calibrate the level of fatigue threshold for propagation. This process is partly shown in Figure 5, in which the numerical numbers indicate the applied shear stress amplitudes, τ_a . The central part of crack that had experienced a relatively high stress of $\tau_a = 800$ -900 MPa exhibited a distinct feature of shear-mode crack growth (cf. B in Figure 5), while the outside that had been subjected to a lower stress of $\tau_a = 640$ -760 MPa showed an irregular crack path accompanied by small bends (cf. A and C in Figure 5), though the crack propagated approximately in the direction of specimen axis without causing a clear branching followed by macroscopic Mode I crack propagation. A large amount of fine oxide-particles was observed, which is considered to be produced by rubbing of opposing crack faces. They are not visible in Figure 5 since most of them had been removed in collecting replicas. In addition, the crack is thicker for the central part shown in B than for the crack tip shown in C probably because the crack faces were worn more by cyclic sliding contact with larger displacement for the central part than for the part near the tip. These results imply that the interference

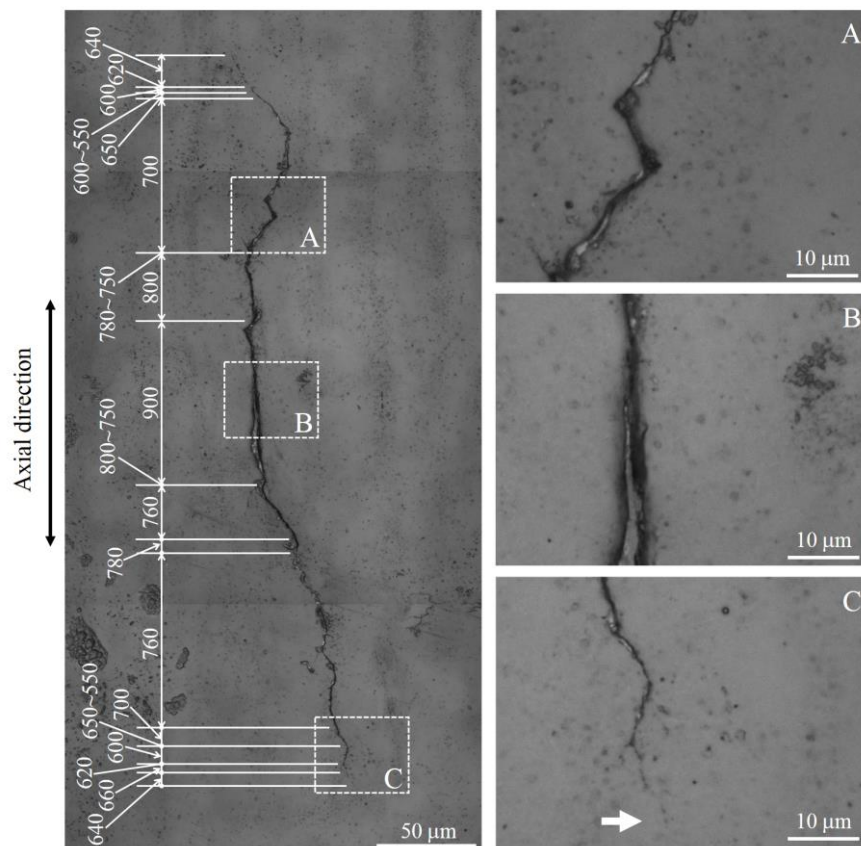


Figure 5. Process of a shear-mode crack growth in τ_a -decreasing test under non-charging condition ($\sigma_s = -1200$ MPa, $f = 20$ Hz). Numbers indicate the applied shear stress amplitude, τ_a , in MPa.

of crack faces would largely affect the shear-mode crack growth behavior. Figure 6 shows the final process approaching the threshold level under the non-charging condition. A slight crack extension is seen but the average crack growth rate, da/dN , is calculated to be 6.4×10^{-12} m/cycle. At this rate, the average increment of crack length per cycle is smaller than the interatomic distance and this means that the crack no longer propagated in a cycle-by-cycle manner. In the present study, therefore, the crack being at this level of growth rate was regarded as a non-propagating crack and accordingly, the applied stress, $\tau_a = 440$ MPa, was defined as the threshold stress, i.e. $\tau_{th} = 440$ MPa.

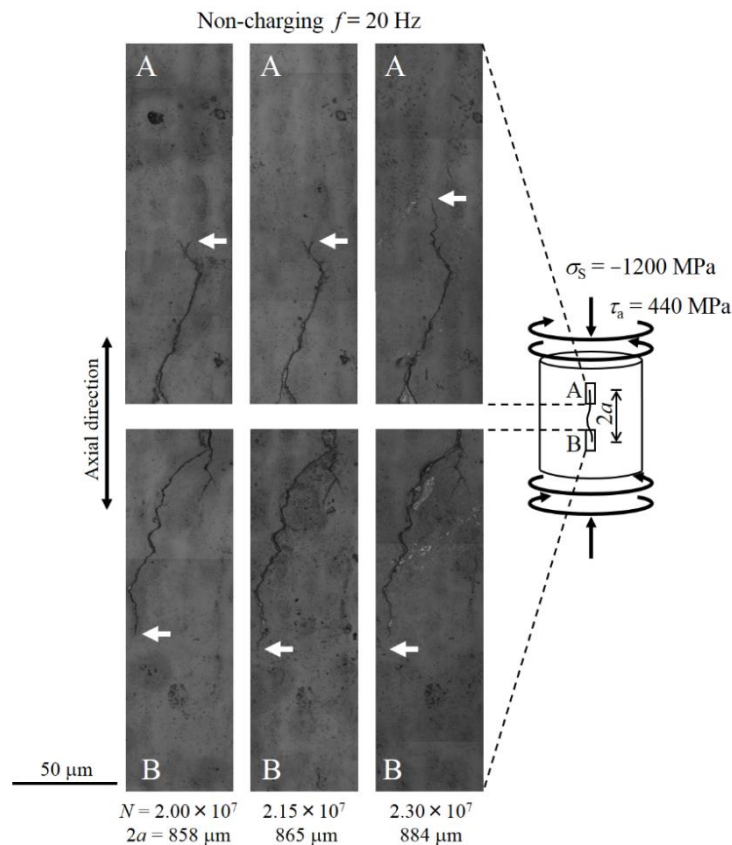


Figure 6. Shear-mode crack growth behavior at threshold level under non-charging condition. ($\sigma_s = -1200$ MPa, $\tau_a = \tau_{th} = 440$ MPa, $f = 20$ Hz)

At step (3), to investigate the influence of hydrogen-charging, the specimen that had been at the threshold level at step (2) under the non-charging condition was next put under the H-charging condition. The mechanical conditions of shear stress amplitude ($\tau_a = 440$ MPa) and statically-applied compressive stress ($\sigma_s = -1200$ MPa) were kept unchanged and only the cyclic frequency was changed from 20 Hz to 2 Hz to facilitate the action of hydrogen. Figure 7 shows the growth behavior of a shear-mode crack under the H-charging condition. It is clearly shown that by hydrogen-charging, the crack growth was reactivated and the growth rate increased to the level of $da/dN = 1.1 \times 10^{-10}$ m/cycle, which is about 170 times greater than the previous growth rate under non-charging condition. The crack path seen in Figure 7 seems to be less irregular compared with that under the non-charging condition at the same stress amplitude level. This may be an indication that hydrogen-charging would facilitate more for shear mode growth than opening mode growth. In our previous [11] and Fujita et al.'s [10] experiments, fatigue tests for almost the same material and testing condition were performed under the high-stress, low-cycle fatigue testing condition, and early initiation of many cracks and

acceleration of crack growth were observed. The present study provides a new result that the hydrogen-charging has also an influence on the low-stress, high-cycle growth behavior of a shear-mode fatigue crack including the threshold condition also in the regime of low stress, high-cycle fatigue. The knowledge of the near-threshold fatigue properties of metallic materials in the presence of hydrogen is considered to become more important in the future. It has previously been uneasy to perform a long-term test for investigation of the effect of hydrogen. However, it is expected that the newly-proposed method of continuous hydrogen-charging would play an important role to the advance of study in this field.

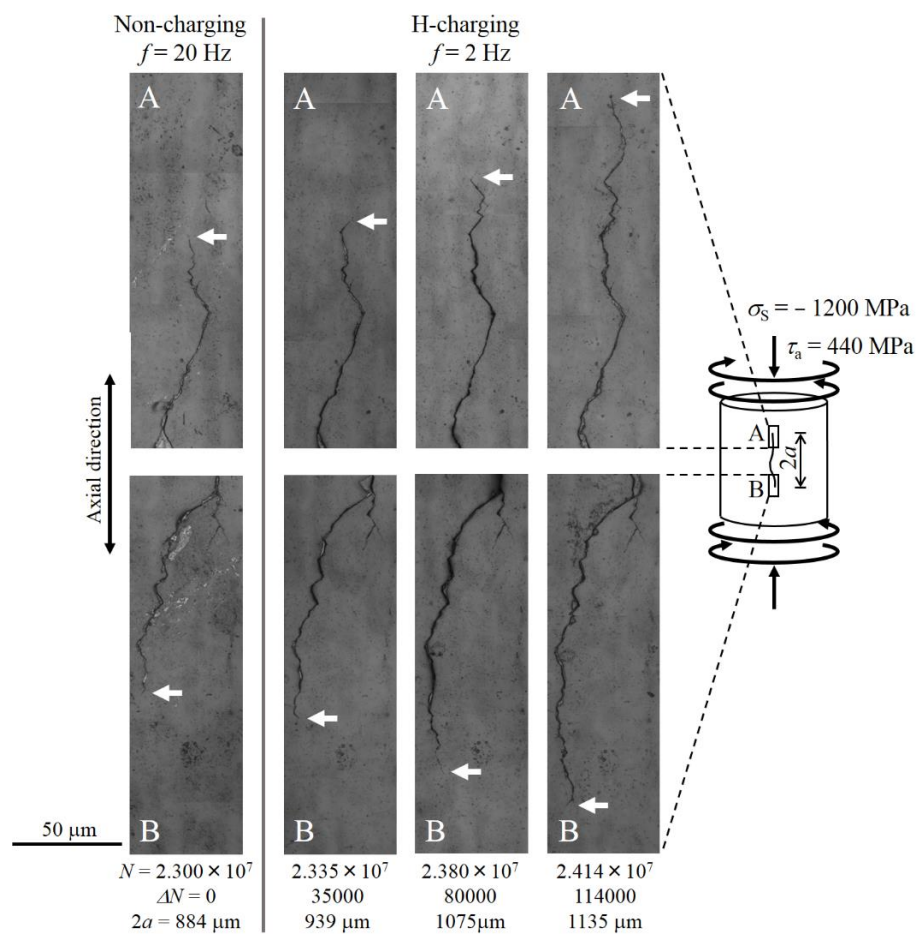


Figure 7. Shear-mode crack growth behavior successively observed after test condition was changed from non-charging to H-charging. ($\sigma_s = -1200$ MPa, $\tau_a = \tau_{th} = 440$ MPa)

4. Conclusions

The shear-mode fatigue crack growth behavior of a bearing steel was observed near the threshold level under the conditions of non-charging and continuous hydrogen-charging. The following results were found:

1. At a high stress of $\tau_a = 900$ MPa under the non-charging condition, a number of shear-mode fatigue cracks initiated at inclusions on the specimens. The stress level was then decreased and finally a threshold stress level of $\tau_{th} = 440$ MPa was obtained.

2. The crack that had been a non-propagating crack under the non-charging condition restarted propagation under the continuous hydrogen charging at the same stress level (i.e. $\tau_a = 440$ MPa). Consequently, the continuous hydrogen-charging affected the growth behavior and reduced the threshold level of a shear-mode fatigue crack.

References

- [1] Tamada K and Tanaka H 1996 *Wear* **15** 245
- [2] Evans M-H. 2012 *Mater. Sci. Technol.* **28** 22
- [3] Matsumoto Y, Murakami Y and Oohori M 2002 *ASTM Bearing Steel Technology* **7** 226
- [4] Evans M-H, Richardson A.D, L. Wang and Wood R.J.K 2013 *Wear* **302** 1573
- [5] Shravan J, Ole W, Peder K and Niels S.J 2015 *Inter. J. Fatigue* **77** 128
- [6] Iso K, Yokouhci A, and Takemura H 2005 *SAE Technical Paper* **114** 1868
- [7] Kino N and Otani K 2003 *JSAE Review* **24** 289
- [8] Matsubara Y and Hamada, H 2006 *J. ASTM. Inter.* **3** 1
- [9] Hamada H and Matsubara Y *NTN Technical Review* **74** 54
- [10] Fujita S, Matuoka S, Murakami Y and Marquis G 2010 *Inter. J. Fatigue* **32** 943
- [11] Akaki Y, Matsuo T, Nishimura Y, Miyakawa S and Endo M 2017 Proceedings of *Damage of Assesment of Structures* To be presented.